The Abdus Salam
International Centre for Theoretical Physics

United Nations
Educational, Scientific and
Cultural Organization

IAEA
International Atomic Energy Agency

**1936-45**

**Advanced School on Synchrotron and Free Electron Laser Sources and their Multidisciplinary Applications**

***7 - 25 April 2008***

**Grazing Incidence Small Angle X-ray Scattering (GISAXS)**

Sigrid Bernstorff
*Sincrotrone Trieste*

Strada Costiera 11, 34014 Trieste, Italy - Tel. +39 040 2240 111; Fax +39 040 224 163 - sci_info@ictp.it, www.ictp.it

# Grazing Incidence Small Angle X-ray Scattering (GISAXS)

*Sigrid Bernstorff*
*Sincrotrone Trieste*
*S.S.14 km 163,5 in Area Science Park, 34012Basovizza (TS), Italy*
*bernstorff@elettra.trieste.it*

## Introduction:

- Scattering with incidence at high angle --> grazing angle: what changes ?
- When is grazing incidence scattering useful ?
- Other grazing incidence techniques:
  - GI X-ray Diffraction
  - X-ray Reflectivity
- Some hints for a good set-up

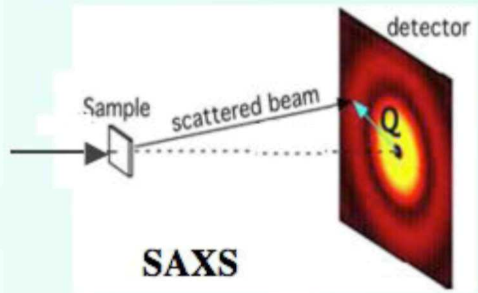


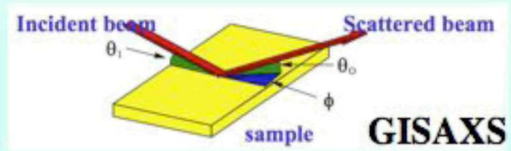


Advanced School on Synchrotron and Free Electron Laser Sources and their Multidisciplinary Applications
07 - 25 April 2008, Trieste, Italy

# The SAXS technique

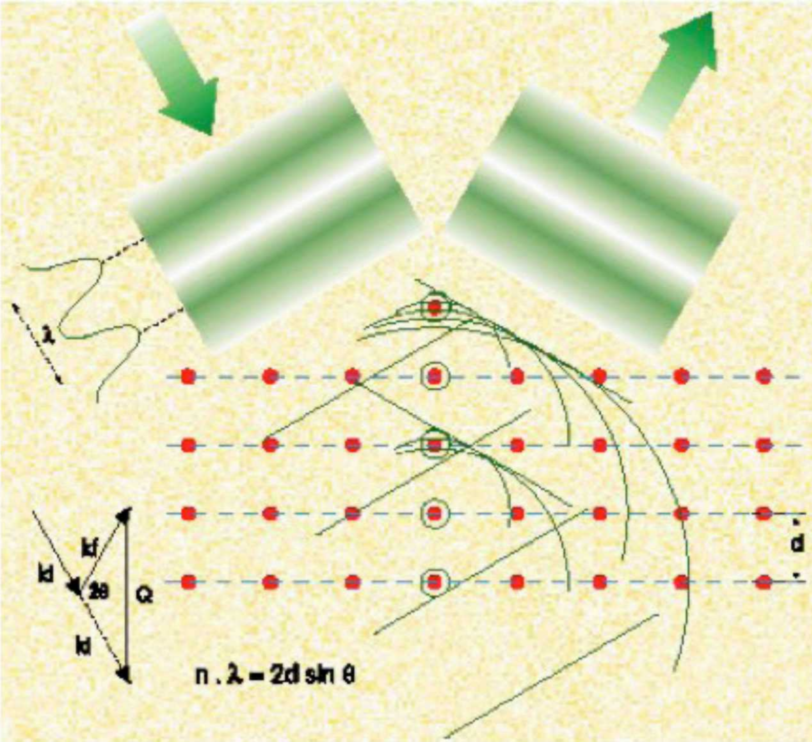


**Bragg's Law**

$$\lambda = 2d \sin\theta$$

**Scattering Vector q**

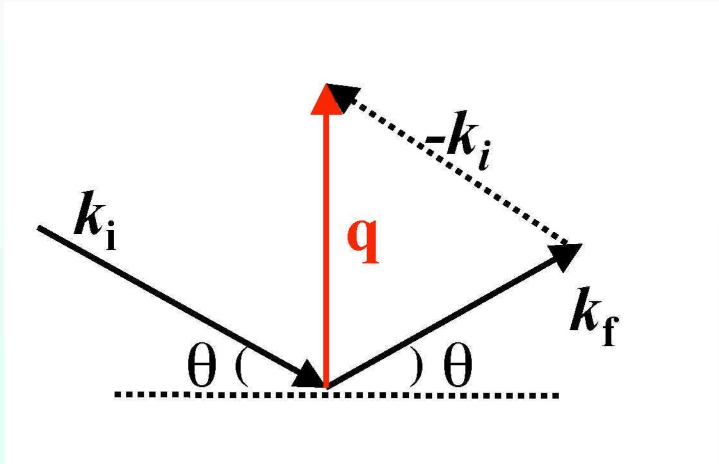


$$q = k_f - k_i = (4\pi/\lambda)\sin\theta$$

$|\mathbf{q}|=2\,k\,\sin\theta$

$q = 2\pi/d$ inverse distance

# Method of Small Angle X-Ray Scattering SAXS

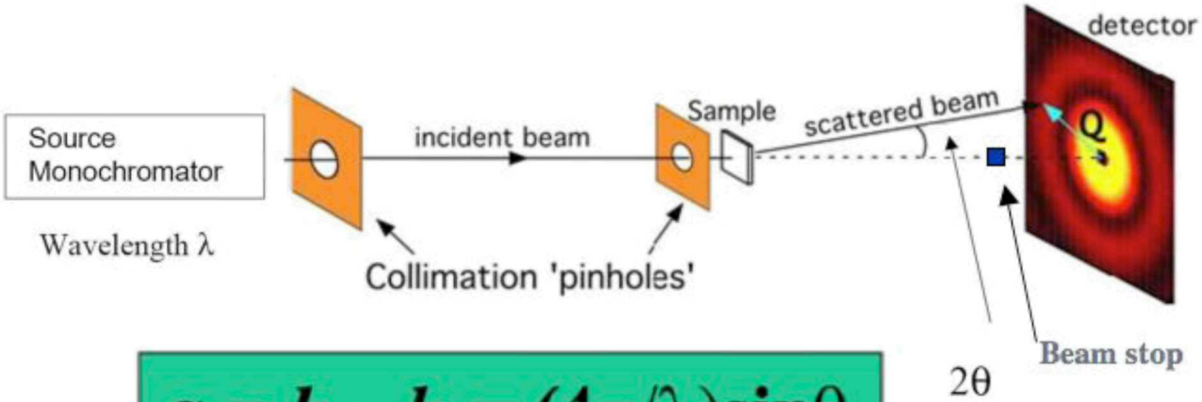


$$\mathbf{q} = \boldsymbol{k_f} - \boldsymbol{k_i} = (4\pi/\lambda)\sin\theta$$

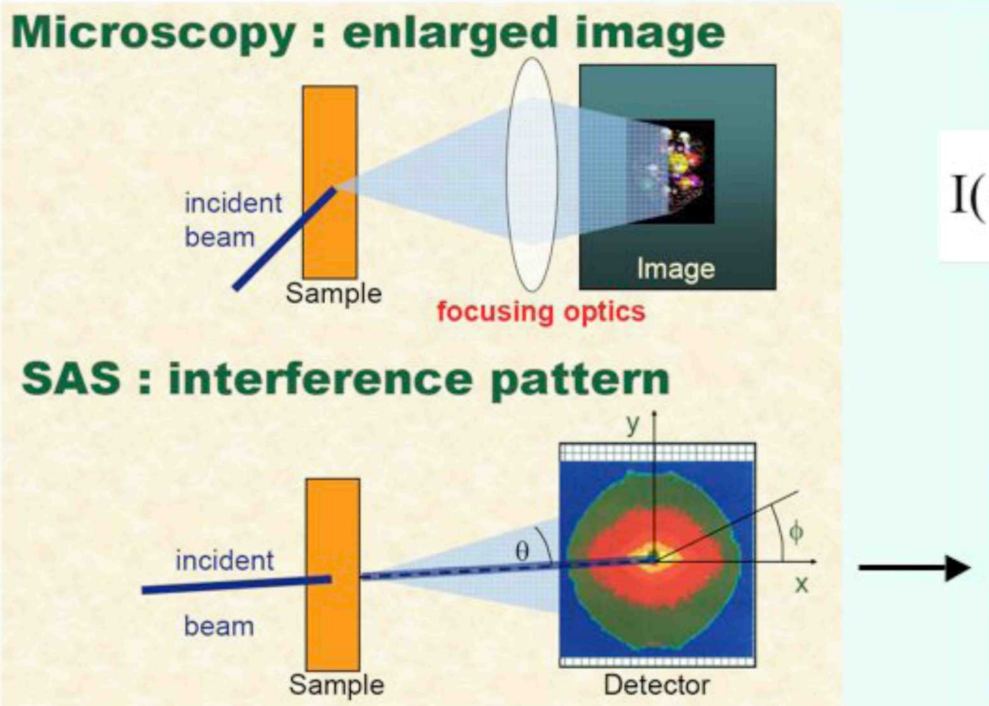


**SAXS intensity**

$$I(q) = \frac{1}{V}\left|\int \rho(r)\, e^{i\,\mathbf{q}\bullet\mathbf{r}}\, d^3r\right|^2 \qquad \rho(r) = \text{electron density}$$

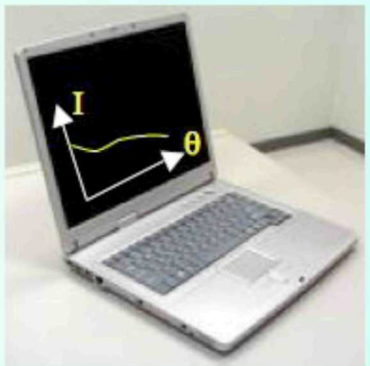

# SAXS technique

$$I(q) = \frac{1}{V}\left|\int \rho(r)\, e^{iq\bullet r}\, d^3r\right|^2$$

$\rho(r)$ = electron density

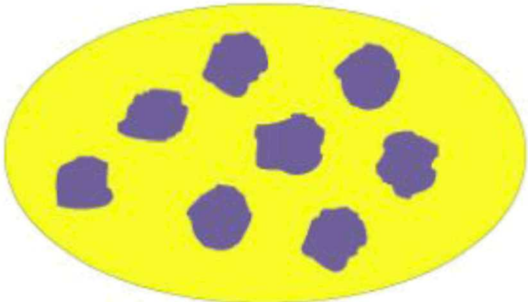

$$I(q) = \frac{N}{V}(\rho_2 - \rho_1)^2 \left|F(q)\right|^2 S(q)$$

$\rho_{1(2)}$ = electron density in phase 1(2)

$|F(q)|^2$: single particle SAXS

$S(q)$: inter particle scattering

**Principle of Babinet :**
pores = particles

$$\int_{V_1} e^{iq\bullet r}\, d^3r$$

# Grazing Incidence Small Angle X-Ray Scattering (GISAXS)

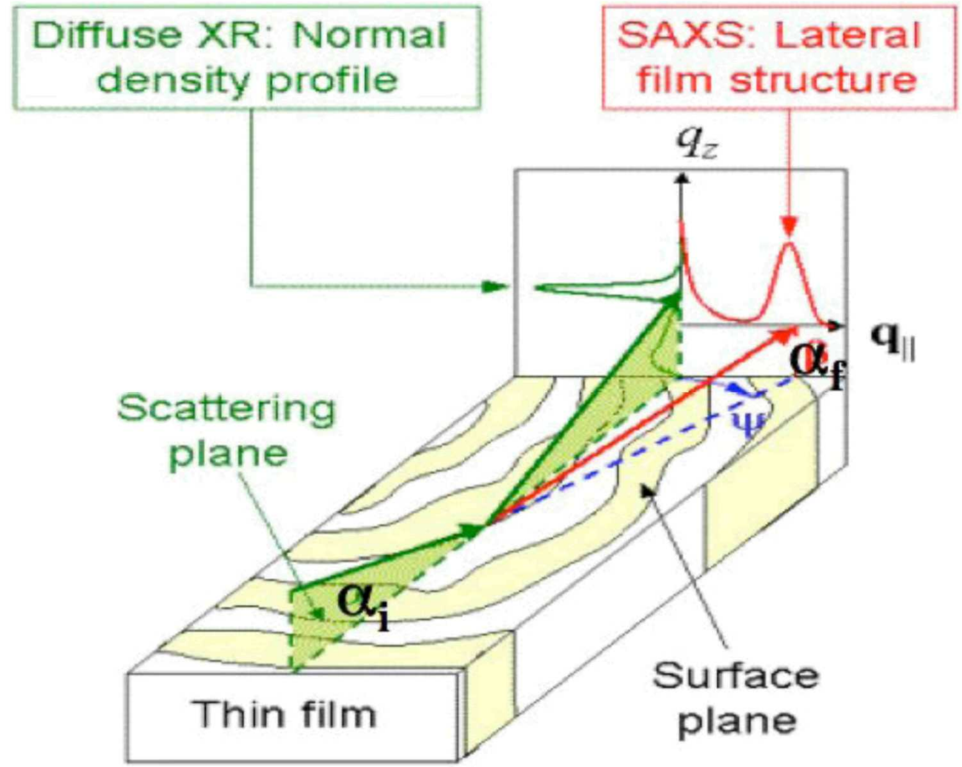


## GISAXS

- combines features from SAXS and diffuse X-ray Reflectivity
- Allows to choose a limited penetration depth -> enhance surface signal (typ. $10^{-6}$ times < substrate scattering)
- is a versatile tool for characterizing average size, shape and particle distance of nano-particles on surfaces, or in thin films

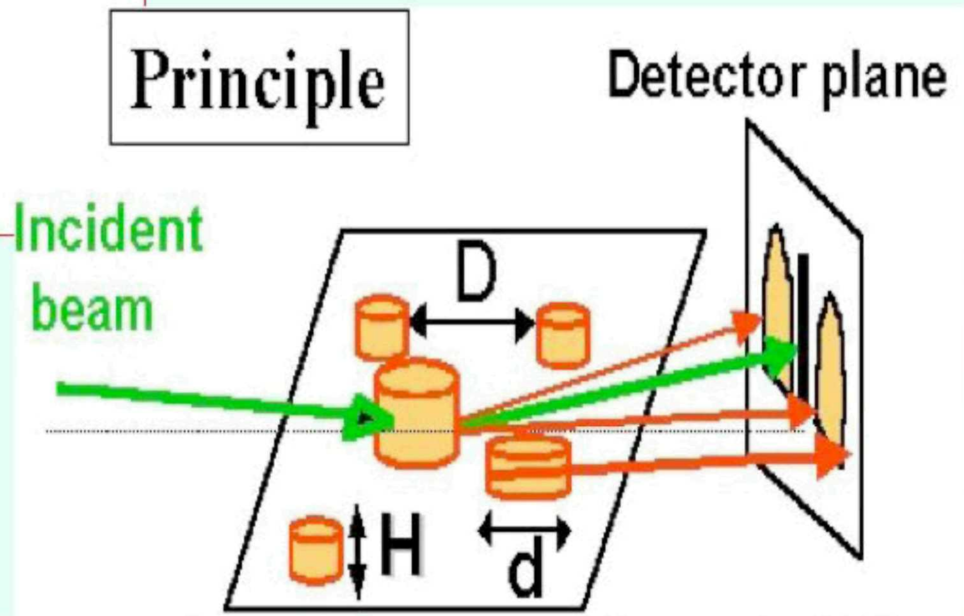


- X-rays are totally reflected under very small grazing angles
- The X-ray grazing angle $\alpha_i$ is chosen between about half the critical angle, $\alpha_C$, and several critical angles

From: Lazzari R., IsGISAXS: a program for grazing-incidence small-angle X-ray scattering analysis of supported islands ,J. Appl. Cryst. 35,(2002) 406

# GISAXS: refraction effects of X-rays

$\alpha_i$ is small ->effects of refraction at the surface needs to be considered:

Refractive index n of matter for x-rays is: $n = 1 - \delta + i\beta$

with:

$$\delta = \frac{1}{2\pi} \times \frac{e^2}{mc^2} \times \frac{N_a \sum_i (Z_i - f_i')}{\sum_i A_i} \times \rho\lambda^2$$

$$\beta = \frac{1}{2\pi} \times \frac{e^2}{mc^2} \times \frac{N_a \sum_i f_i''}{\sum_i A_i} \times \rho\lambda^2 = \mu \frac{\lambda}{4\pi}$$

$$= 2.701 \times 10^{-6}\, x \frac{\sum_i (Z_i - f_i')\ [\text{el. units}]}{\sum_i A_i\ [\text{g / mol}]} \times \rho\, [\text{g/ cm}^3]\, \lambda^2 [A^2]$$

summation over all atomic species i:

$(Z_i - f_i')$ scattering factor

$f_i''$ anomalous dispersion factor

$A_i$ atomic weight

$N_a$ Avogadro's number

$\rho$ density

$\lambda$ wave length

$\mu$ photo electric absorption coefficient

# GISAXS: refraction effects of X-rays

**Refractive index $n = 1 - \delta + i\beta$**

**critical angle of total reflection $\alpha_c \propto \sqrt{2\delta}$**

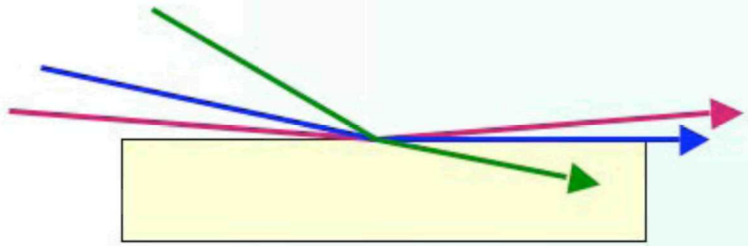

**Typical orders of magnitude:**

$\delta \approx 10^{-5}$ (10 keV)

$\beta \approx 10^{-6}$

$\alpha \approx 0.1^0 - 0.5^0$

**Note:**

- **Real part of $n = 1 - \delta + i\beta$ is always slightly < 1**
- **Because of refraction, a beam passing from vacuum into a sample comes closer to the sample surface**
- **For $\alpha_i < \alpha_c$, the beam is totally reflected, and only an evanescent wave, which decays over some nm, is present below the surface**
- **For $\alpha_i > \alpha_c$ the transmitted wave propagates**

# Scattering Depth

The perpendicular components of the incident and emergent wave vectors are modified upon crossing the surface, and become complex due to refraction and absorption:

$$k'_{i,f_\perp} = \frac{2\pi}{\lambda}(A_{i,f} - iB_{i,f})$$

For small incidence and emergence angles:

$$A_{i,f} = \frac{1}{\sqrt{2}}\left(\sqrt{(\alpha_{i,f}{}^2 - \alpha_c{}^2)^2 + 4\beta^2} + \alpha_{i,f}{}^2 - \alpha_c{}^2\right)^{0.5}$$

$$B_{i,f} = \frac{1}{\sqrt{2}}\left(\sqrt{(\alpha_{i,f}{}^2 - \alpha_c{}^2)^2 + 4\beta^2} + \alpha_c{}^2 - \alpha_{i,f}{}^2\right)^{0.5}$$

-> the perpendicular momentum transfer $Q'_\perp = k'_{f\perp} - k'_{i\perp}$ inside the sample becomes complex

The scattering depth $\Lambda = \frac{1}{\mathrm{Im}(Q'_\perp)} = \frac{\lambda}{4\pi(B_i + B_f)}$ is thus strongly affected by refraction when $\alpha_i$ and / or $\alpha_f$ are close to $\alpha_c$

# Refraction effects

**Scattering depth** $$\Lambda = \frac{1}{\mathrm{Im}(Q'_\perp)} = \frac{\lambda}{4\pi(B_i + B_f)}$$

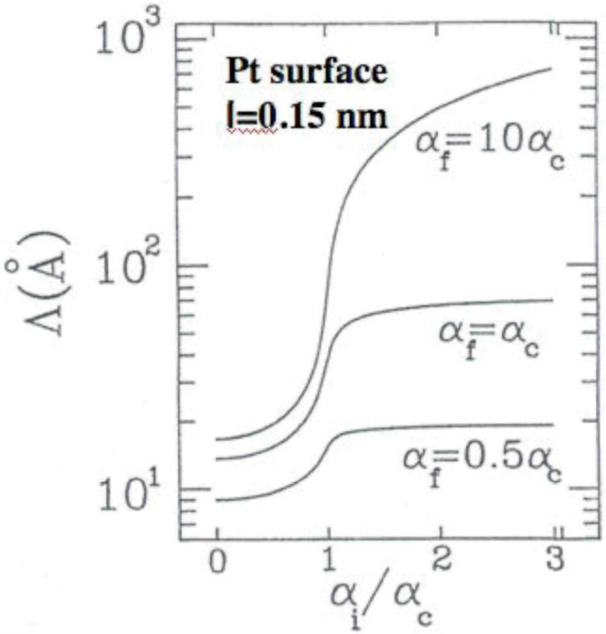


**The reflection and transmission coefficients are also strongly affected by refraction when $\alpha_i$ and / or $\alpha_f$ are close to $\alpha_c$ :**

$$R_{i,f} = \frac{\alpha_{i,f}^{\;2} - 2\alpha_{i,f} A_{i,f} + A_{i,f}^{\;2} + B_{i,f}^{\;2}}{\alpha_{i,f}^{\;2} + 2\alpha_{i,f} A_{i,f} + A_{i,f}^{\;2} + B_{i,f}^{\;2}}$$

$$T_{i,f} = \frac{4\alpha_{i,f}^{\;2}}{\alpha_{i,f}^{\;2} + 2\alpha_{i,f} A_{i,f} + A_{i,f}^{\;2} + B_{i,f}^{\;2}}$$

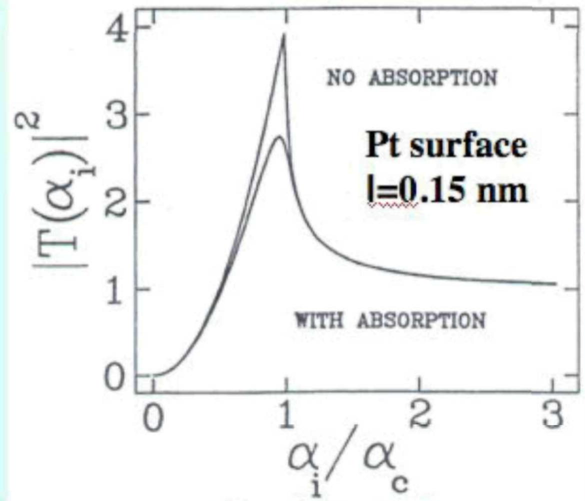


**$R_{i,f} = 1$ for $\alpha_{i,f} < \alpha_c$ (regime of total reflection)**
**T = 4 (max value) at $\alpha_c$**

**-> use $\alpha_i$ and / or $\alpha_f$ close to $\alpha_c$ to enhance surface scattering !**

*G. Renaud/Surface Science Reports 32 (1998) 1–90*

# Example: Quantum Dots studied by GISAXS

### II-VI semi-conductors Nanostructures: what for ?

**quantum confinement of excitons,**
**increase of the energy gap**

↓

- **variable length optical absorbers**
- **high-speed non-linear optical switches**
- **photoluminiscence with variabel wavelength by changing particle size ( -> quantum dot laser)**
- **formation of nanoparticles in dielectrics and non-absorbing materials**

**BUT: working devices will depend on a precise control of size and density of an ensemble of Quantum Dots (QD)!**

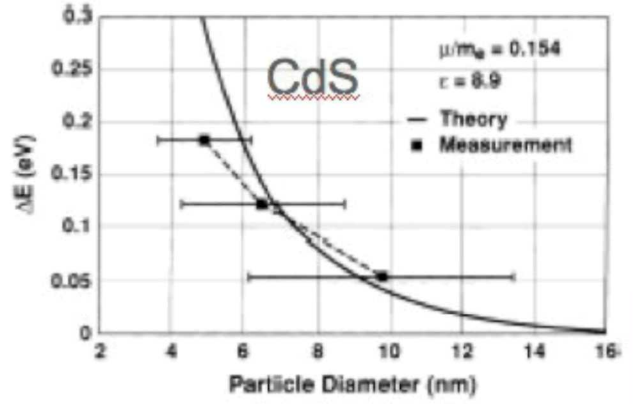


Fig. 5. Calculated and measured bandgap shift for CdS nanocrystals. The solid line is calculated from Eq. (2). The points are measurements of the bandgap shift from Eq. (1) for the samples in Fig. 4.

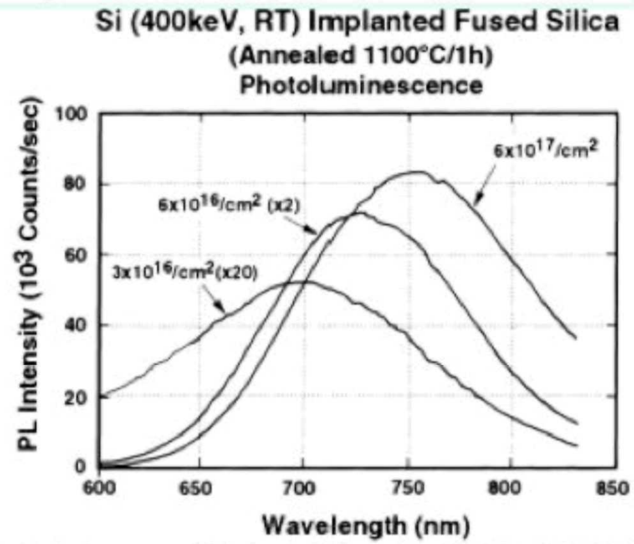


*C.W. White et al. / Nucl. Instr. and Meth. in Phys. Res. B 141 (1998) 228*

# Nanocrystals in Substrates

**Schematic of the ion implantation technique for NC production**

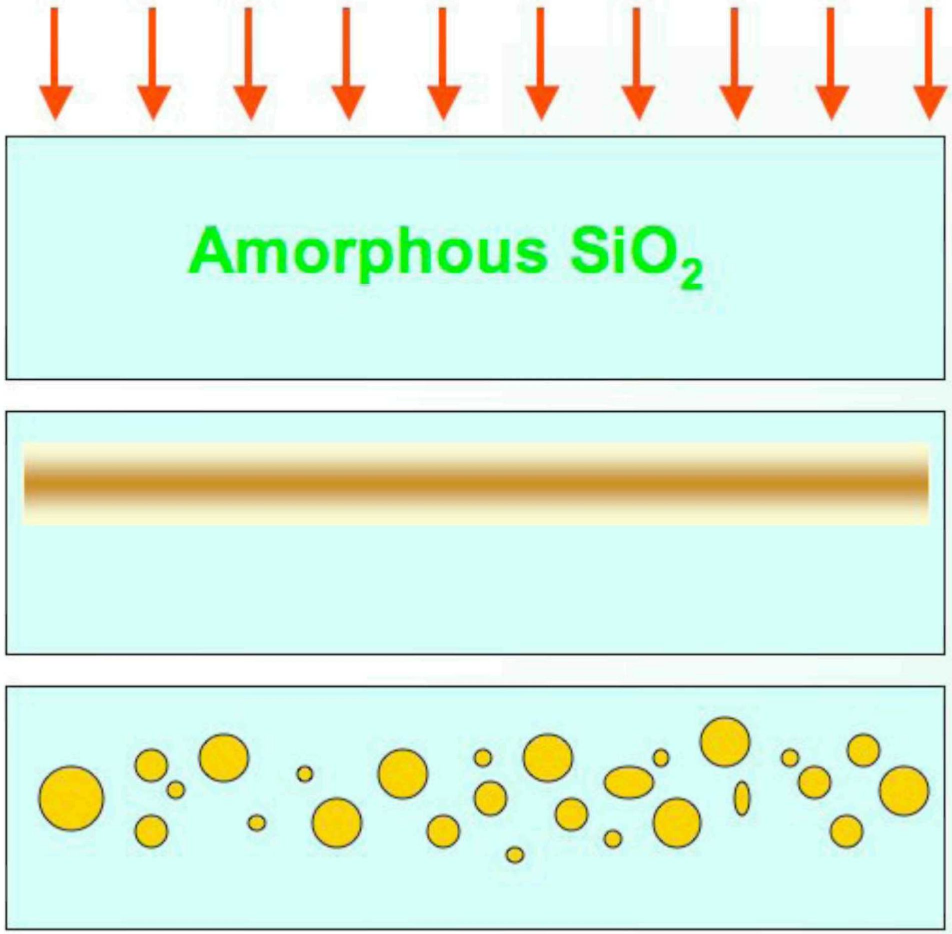


**(a) Host material *implanted* with equal doses of group II and VI ions**

**(b) *Supersaturated solid solution* formed in the near surface region**

**(c) *nucleation of precipitates,* precipitates *grow* on the expense of incoming ion flux**

**d) during high-T annealing II-VI nanoparticles are being synthesized and in the process of Ostwald ripening agglomerating in discrete, isolated QD's of varying size**

# GISAXS: what information do we get ?

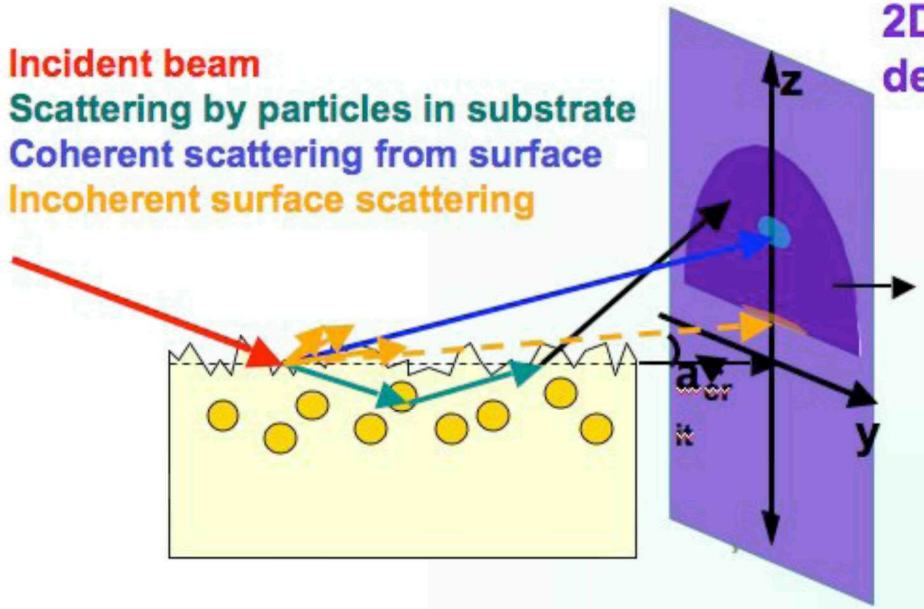


2D GISAXS pattern

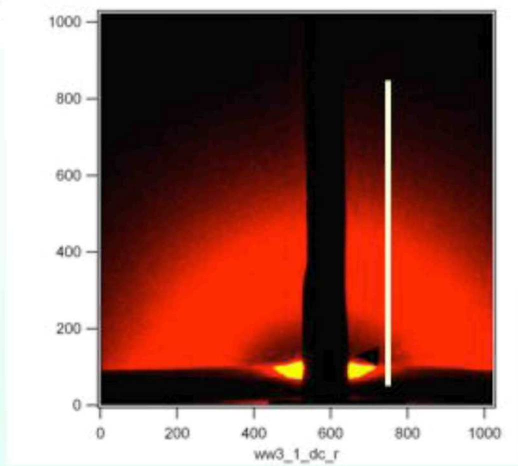


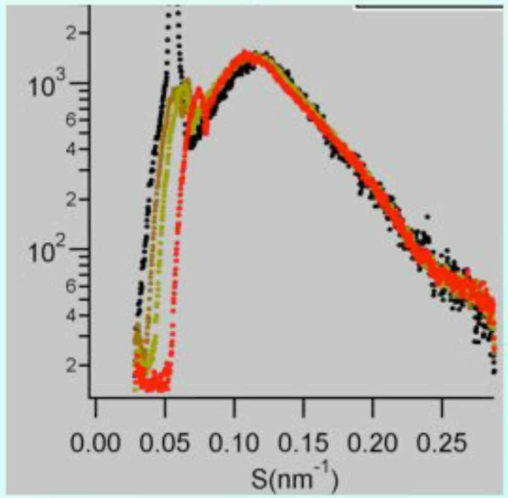


$\Lambda = 2\pi/q_m$, $\Lambda$ = average nanocrystals distance - obtained from interference peak, $q_{max}$

$R_g$ = radius of gyration

$\Rightarrow$ D = average cluster diameter obtained from slope of linear region of **I(*q*) versus *q*²**

U.V. Desnica, P. Dubcek, I.D. Desnica-Frankovic, M. Buljan, S. Bernstorff and C.W. White, J.Appl.Cryst. 36, 443-446 (2003)

# Synthesis and growth of CdS Quantum Dots in $SiO_2$

**GISAXS-pattern** **Intensity profiles**

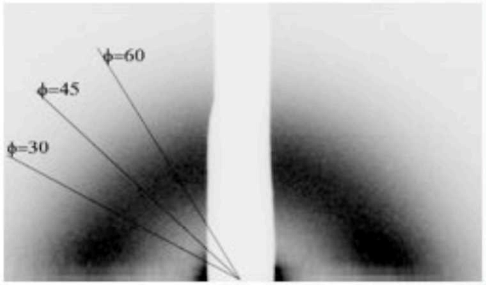


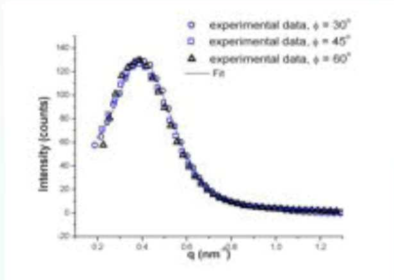


→ Isotropical distribution of spherical QDs with average diameter 8.8 nm, and with average distance of 10.8 nm

Concentration 5.3 exp 21/cm$^3$

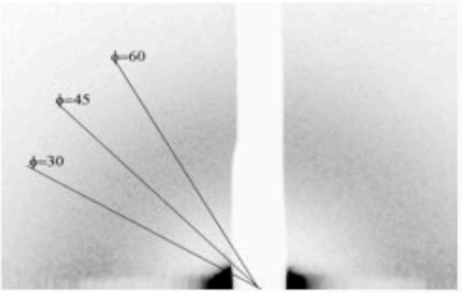


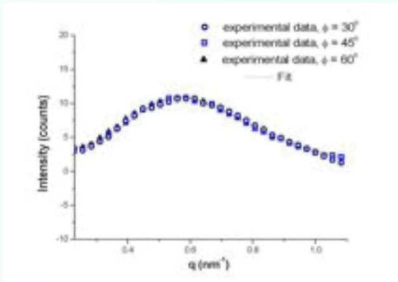


→ Isotropical distribution of spherical QDs with smaller average diameter and larger distance

Concentration 2.0 exp 21/cm$^3$

LMA approximation, and DWBA formalism -> scattered intensity is:

$$I(q) \propto \left|T(\alpha_i)\right|^2 \left|T(\alpha_f)\right|^2 \int_0^\infty P(q,D) S(q, D_{hs}, \eta_{hs}) N(D,w)\, dD$$

U.V. Desnica, P. Dubcek, I.D. Desnica-Frankovic, M. Buljan, S. Bernstorff and C.W. White, J.Appl.Cryst. 36, 443-446 (2003)

# GISAXS data evaluation

**Scattering from embedded particles: Local Monodisperse Approximation - LMA**

**-system is approximated by monodisperse subsystems, weighted by the size distribution**
**-positions of the particles are completely correlated with their sizes**

$$I(q) \propto \left|T(\alpha_i)\right|^2 \left|T(\alpha_f)\right|^2 \int_0^\infty P(q,D) S(q, D_{hs}, \eta_{hs}) N(D,w)\, dD$$

**$T(\alpha_i)$ and $T(\alpha_f)$ - Fresnel transmission coefficients for angle of incidence $\alpha_i$ and exit $\alpha_f$**

**P(q,D) - form factor of a homogeneous sphere of diameter D, (D=2R);**

**$S(q,D_{hs},\eta_{hs})$ - structure factor ($\eta_{hs}$ - volume fraction and diameter of the hard spheres)**

**N(w,D) - Gaussian size distribution function**

**Surface Scattering: Distorted Wave Born Approximation - DWBA**

$$I_{total} = I_{LMA} + I_{surface}$$

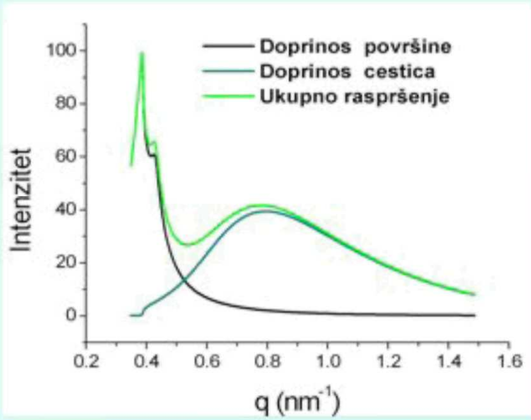



**Distorted Wave Born Approximation:**
Vineyard 1982, Shinha et al. 1988
M. Rauscher, T. Salditt and H. Spohn, Phys. Rev. B 52, 16855 (1995)
M. Rauscher et al., J. Appl. Phys. 86 (12), 6763 (1999)

# Quantitative analysis of GISAXS

$$I(q_{//}, q_{\perp}) \approx \left\langle |F|^2 \right\rangle \times S(q_{//})$$

*Is*GISAXS program :
http://www.esrf.fr/computing/scientific/joint_projects/IsGISAXS/
R. Lazzari, J. Appl. Cryst. 35, 406 (2002)
F. Leroy, R. Lazzari and G. Renaud, Acta. Cryst. A 60, 565, (2004)

*Form factor :*
a kind of shape FT
with refraction effects

×

*Interference function:*
FT of pair
correlation function

$$S(q_{//}) = 1 + \rho_S \int \left(g(r) - 1\right) e^{-iq_{//} r} d^2 r$$

$$F_{DWBA}(q_{//}, k_i, k_f)$$

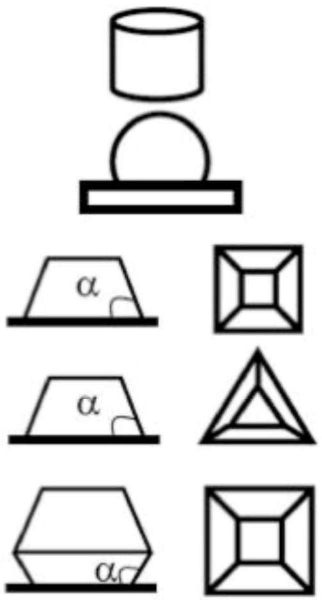


•Cylinder
•Troncated sphere
•Pyramid
•Tetraedron
•Cubooctaedron

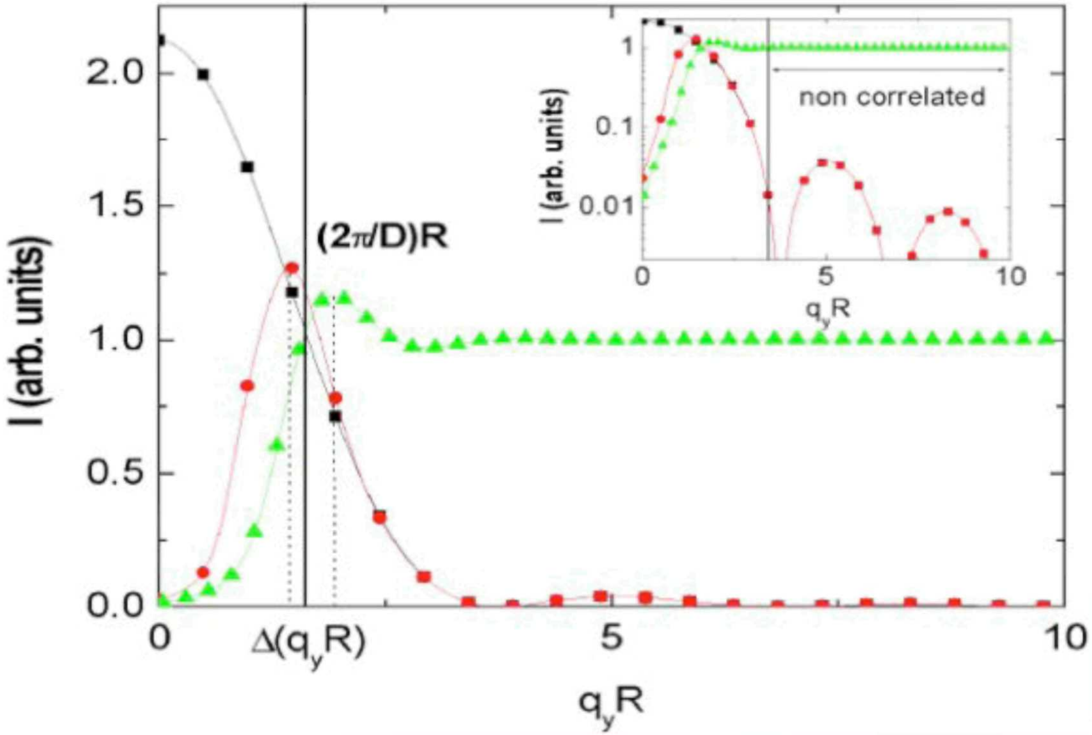

# Synthesis and growth of CdS Quantum Dots in $SiO_2$

## GISAXS

(grazing angle 2.25° ) vs. total scattering angle.

**Yoneda Peak**

(at $\alpha_c$, due to the maximum in the Fresnel transmission function)

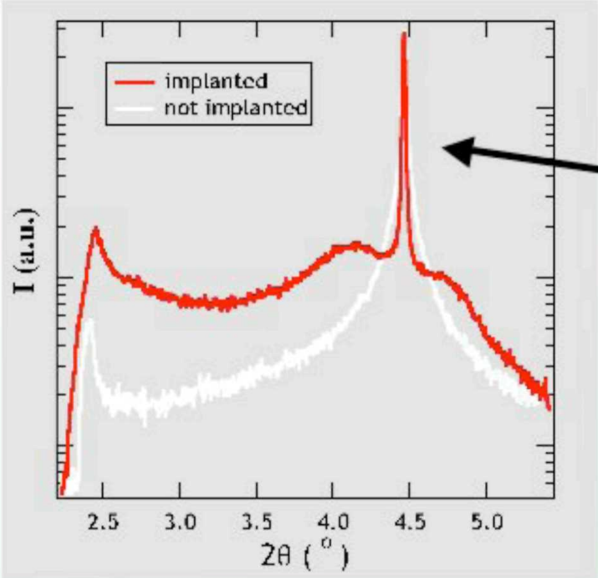


**Sharp specular peak**

(due to Fresnel reflectivity)

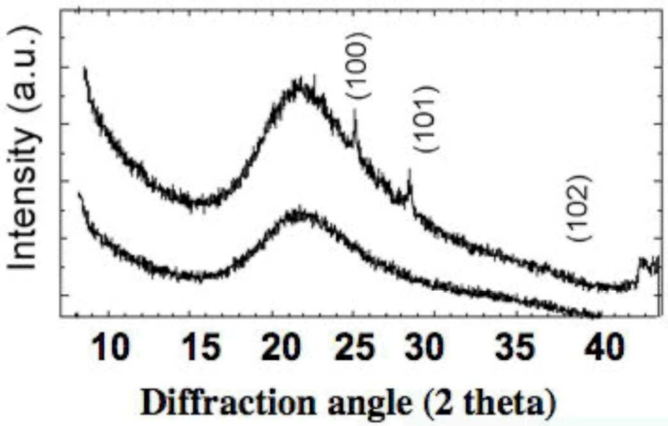


## X-ray Diffraction

- Broad signal from amorphous $SiO_2$ substrate
- Superimposed: sharp peaks identified as CdS (hexagonal)
- Determination of average nanocrystal size (from the broadening of lines)

# Bimodal size distribution of particles: GISAXS + TEM

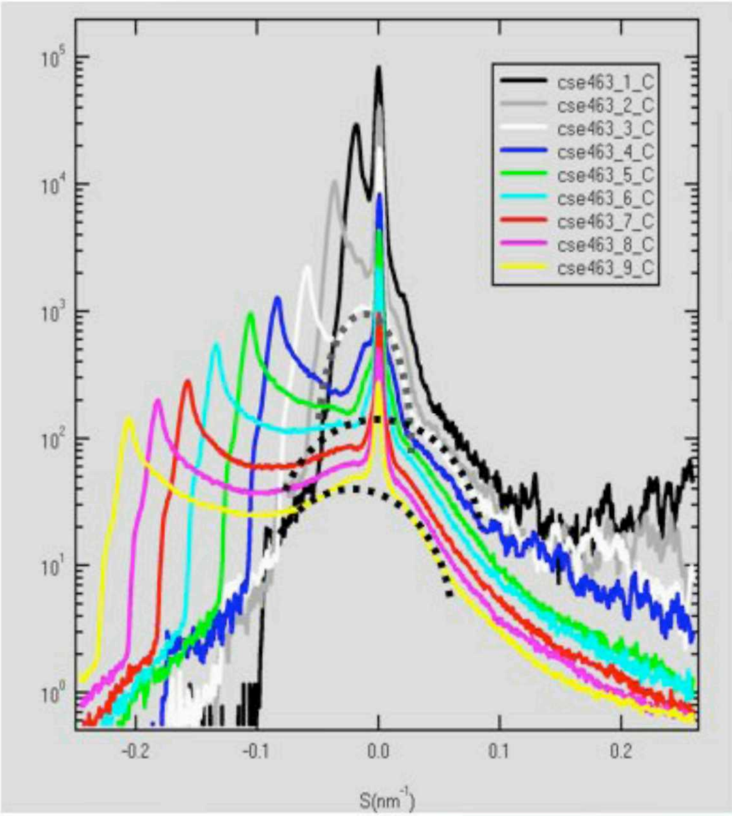


→ depth profiling by small increase of the incidence angle (0.02° step)

closely spaced population of large particles with narrow size distribution $R_G \approx 50$ -60 nmnm

shoulder - second group of smaller particles of broader size distribution $R_G \approx 5$-7 nm

(**CdSe in $SiO_2$**, +0% Cd, 800 °C in Ar+$H_2$)

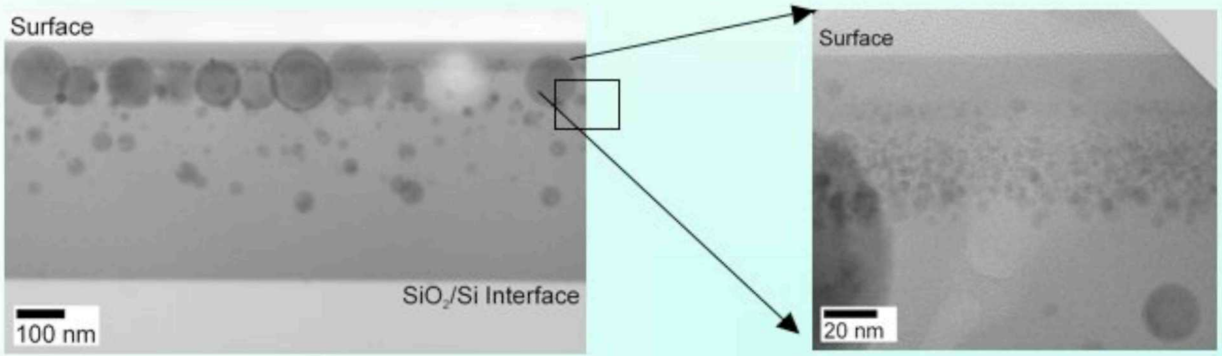


Cross-sectional **TEM** image:

Size distribution for **ZnSe nanocrystals in $SiO_2$** after annealing at 1000 °C, 30s, Ar. Sample was implanted with 33% surplus Cd. Among large particles positioned at approx. 100nm, there is also a band of small particles with diameters below 10 nm

U.V. Desnica, M. Buljan, I.D. Desnica-Frankovic, P. Dubcek, S. Bernstorff, M. Ivanda et al, NIM B 216, 407 (2004)

# Complementary Methods

## GISAXS:

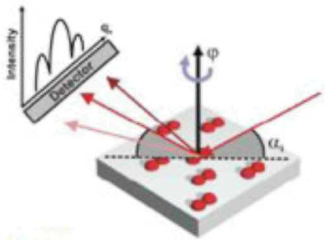


- averages over macroscopic areas, but still yields microscopic information
-- lateral and vertical correlations
-- intrinsically sensitive to strain
-- information about buried objects
- gives reciprocal space information: GISAXS is an indirect method, to find proper models for the data evaluation is crucial
- width of Bragg peaks in X-ray scattering depends not only on the size of the crystalline regions but also on their perfection

## Microscopy (AFM, STM, ...):

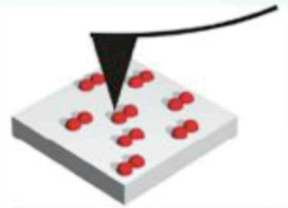

- sees shape of QD (faceted pyramids, hut clusters, dome-like structures, ...)
- gives real space surface images
- too small sampling statistics for getting size distribution and ordering effects
- strain cannot be detected
- buried dots are not accessible

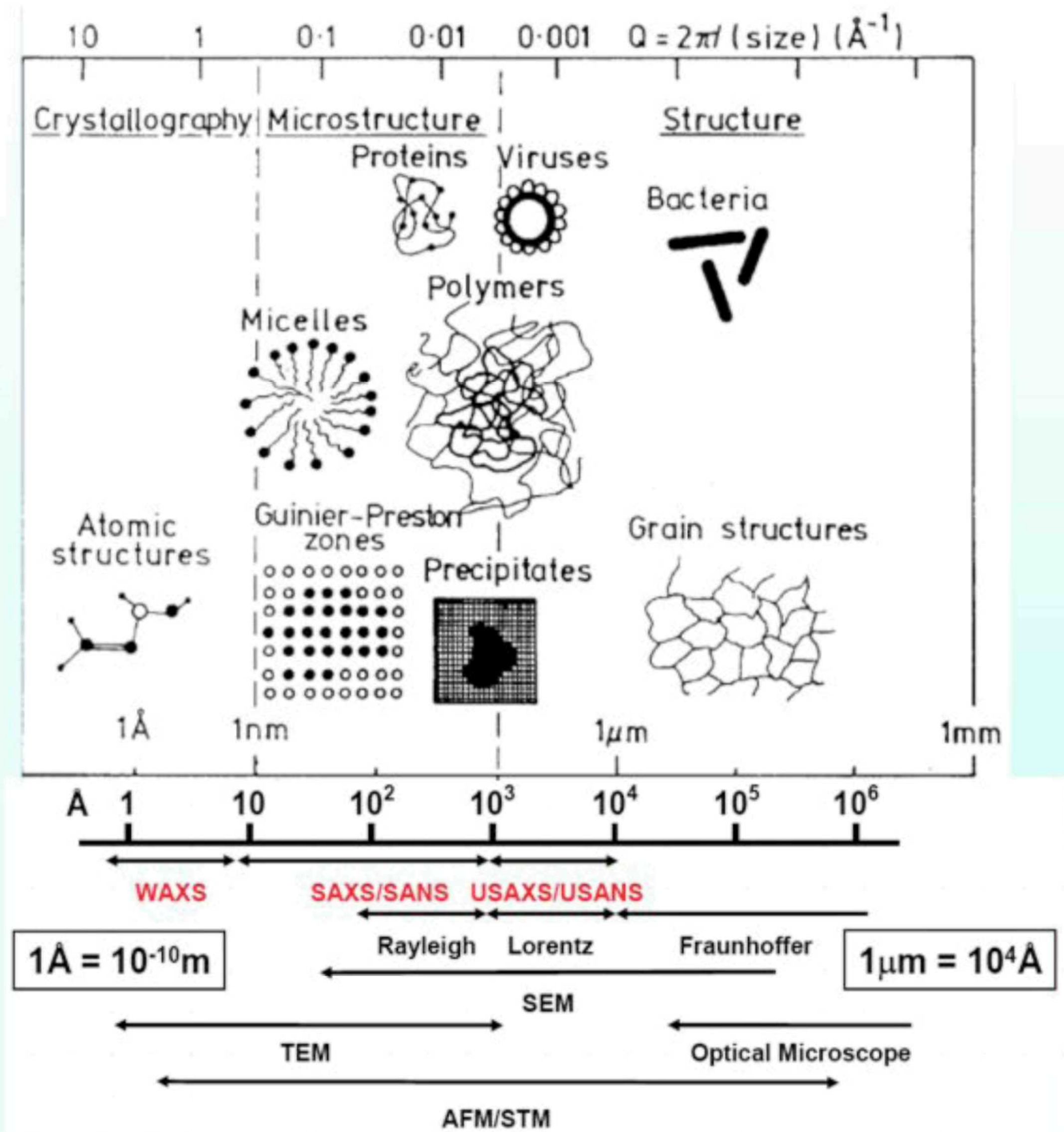

# GISAXS study of Ge islands on a Si(111) substrate

Sample prepared by molecular beam epitaxy at substrate temperature 530°C

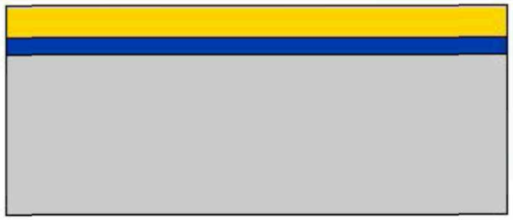

15 nm Ge

1/3 layer Boron ( $\sqrt{3} \times \sqrt{3}$ reconstruction on Si (111))

150 nm Si

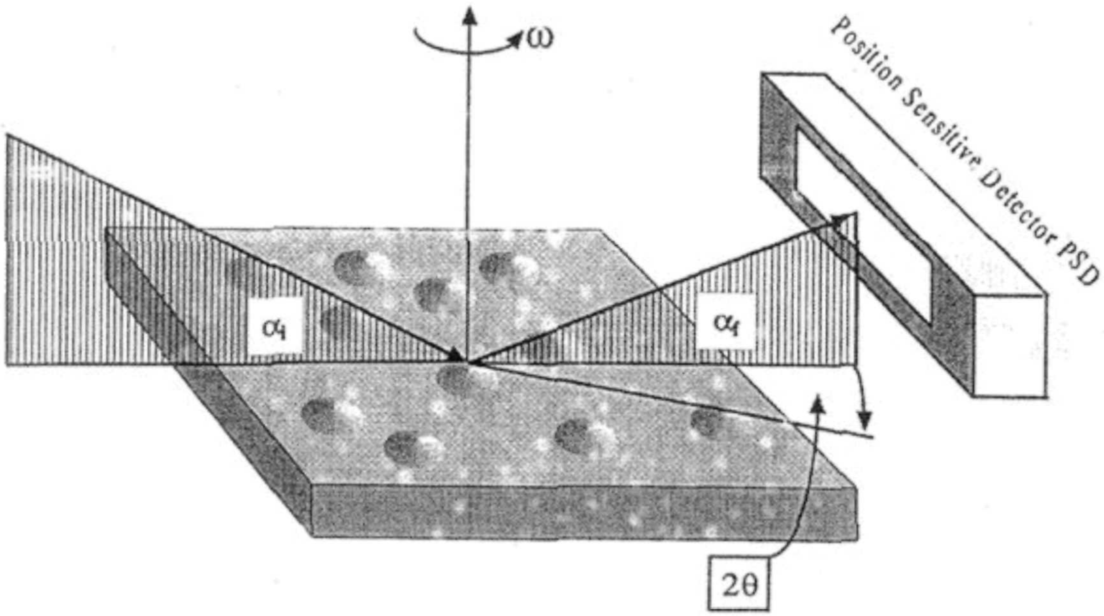


Rotate azimuthal angle $\varpi$ keeping all other angles unchanged -> axial symmetry of QD since $q_z \neq 0$

Not possible with transmission SAXS ( $q_z = 0$ ) !

Scattering geometry for grazing incidence small angle scattering (GISAXS). The PSD is placed parallel to the sample surface : collects the small angle signal as a function of $q_\parallel = 2\pi/\lambda \sin(2\theta)$ at constant angles of incidence and exit, $\alpha_i \neq \alpha_f$. The axial symmetry the quantum dots are studied by rotating the azimuthal angle $\omega$.

T.H. Metzger et al., J. Phys D: Appl. Phys 32 (1999) A202-A207

# GISAXS study of Ge islands on a Si(111) substrate

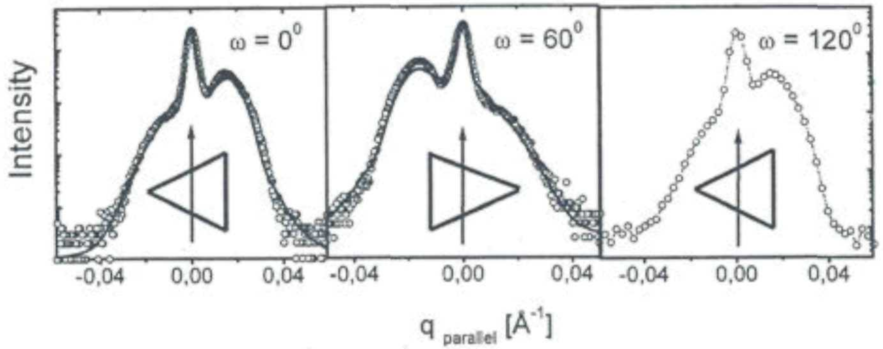


GISAXS signal from Ge pyramids on Si(111) for different azimuthal angles as a function of $q_\parallel$. The pyramids possess a threefold symmetry. The full curve is a fit to the experimental data (OOOO) using the structure factor of a pyramid

**3-fold symmetry of scattering pattern**

**means**

**3-fold symmetry of triangular pyramids**

- **Relation of ϖ and known cleavage edge direction of the sample -> sides of pyramids are aligned along all possible <110> directions in the (111) oriented surface plane**
- **Fit of structure factor to experimental data -> dimensions of the pyramids**


**AFM (atomic force microscope) -> islands have pyramidal shape with well defined {113} facets; some exhibit also a small (111) terrace on a truncated top**

T.H. Metzger et al., J. Phys D: Appl. Phys 32 (1999) A202-A207

# Towards Quantum Dot Laser: the samples

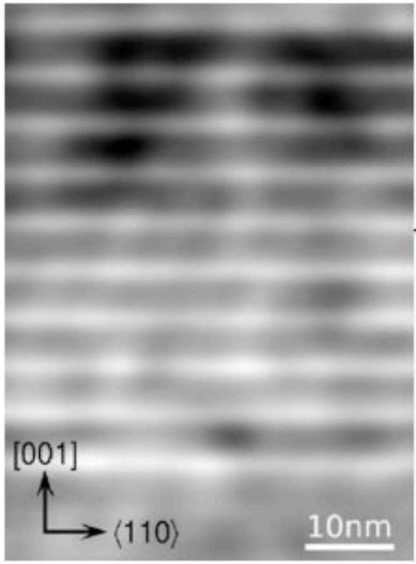


14.5 nm average QD distance

Z-contrast cross section TEM for 10-fold stack sample (QD layers: 0.6 nm, spacer: 4.2 nm $T_{growth}$ = 280 °C

N QD containing CdSe layers

N+1 strain compensating ternary spacer layers of thickness d

Cap layer

Buffer layer

Substrate

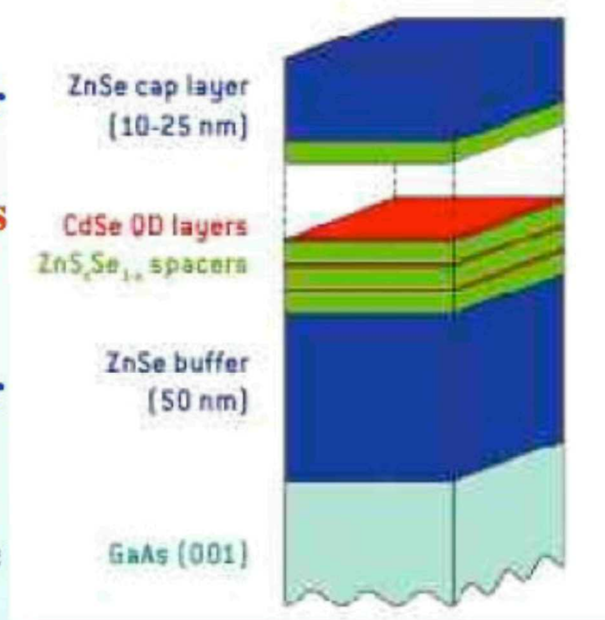


Samples grown by migration enhanced molecular beam epitaxy with:

N = 3, 5 or 10

CdSe layers thickness: 1.8 monolayers (i.e. 0.5-0.6nm)

$d_{spacer}$ = fix value in the range 2.0 nm - 8.0 nm

Substrate temperature: 230, 280 or 310 °C

Th. Schmidt et al., Physical Review B72, 195334 (2005)

# GISAXS reveals CdSe/ZnSSe Quantum Dot ordering

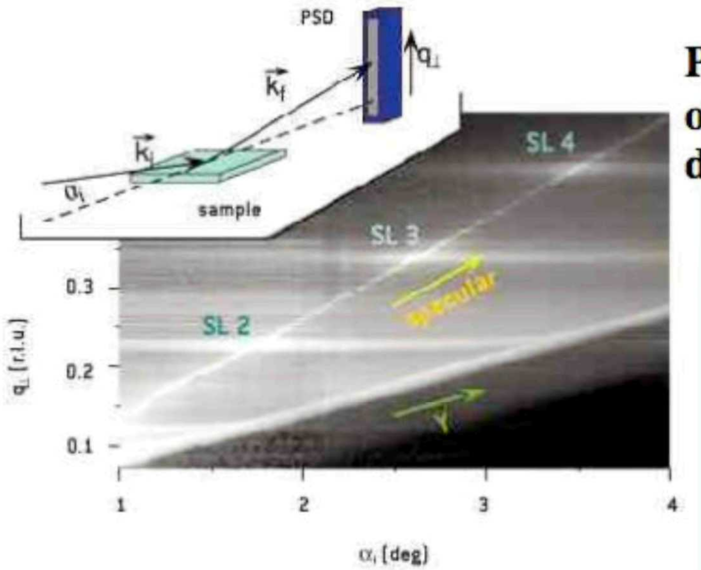


Pseudo 2D presentation of 1D spectra taken in dependence of $\alpha_i$

Bragg peaks of super lattice

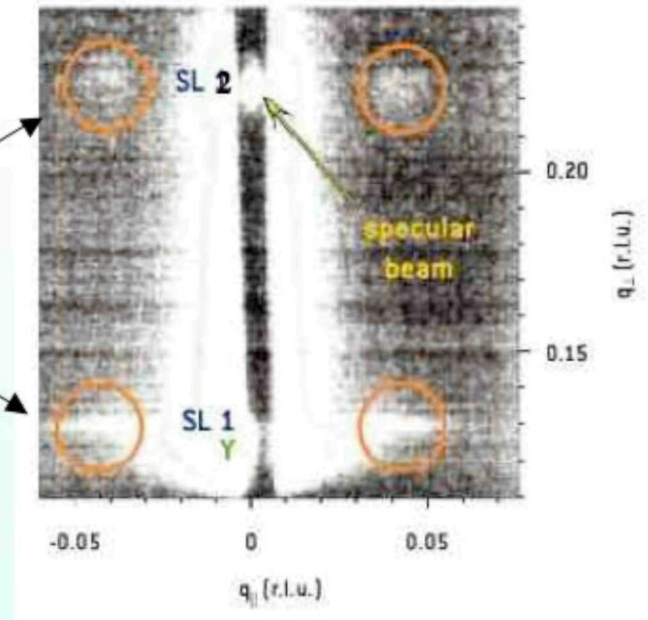


2D GISAXS pattern taken at $\alpha_i = 1.4^o$

**QD superlattice:** degree of ordering depends strongly on growth parameters.

High ordering for:
- Many QD layers
- Adequate layer thickness
- High growth T

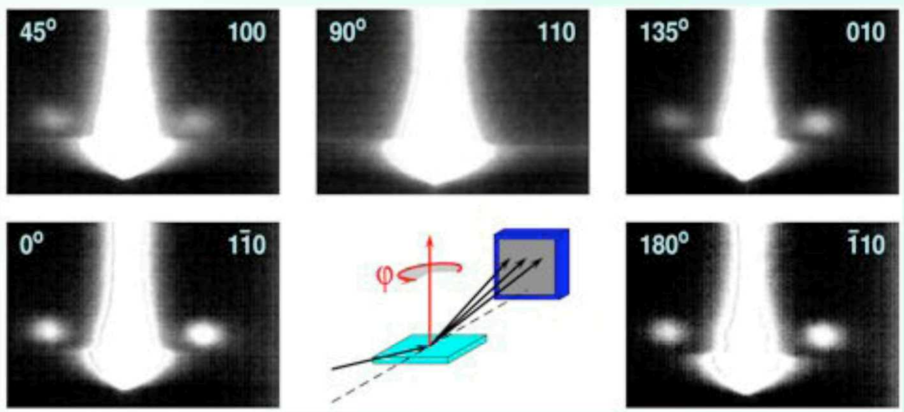


10 QD layers a 0.6 nm
4.2 nm spacer
$T_{growth}$ = 280 °C

14.5 nm average QD distance, shape anisotropy

Th. Schmidt et al., Physical Review B72, 195334 (2005)

Th. Schmidt, T. Clausen, J. Falta, G. Alexe, D. Hommel, S. Bernstorff, *Elettra Highlight 2004, p. 63*

# Grazing Incidence Diffraction (GID)

**<u>Scattering geometry:</u> defined by directions of incident beam and detector position**

**To reach <u>diffraction condition</u>: rotate sample about its surface normal so that net-planes make angle Θ with respect to both incident and scattered beam -> probe long range periodicity parallel to sample surface**

**To see <u>reflected beam</u>: $\alpha_i = \alpha_f$ , $2\,\Theta = 0$**

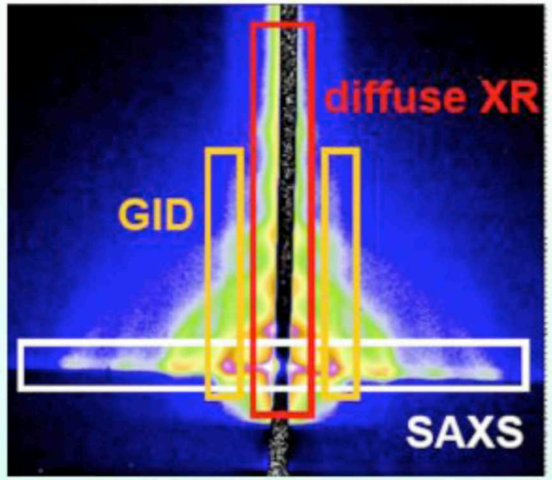


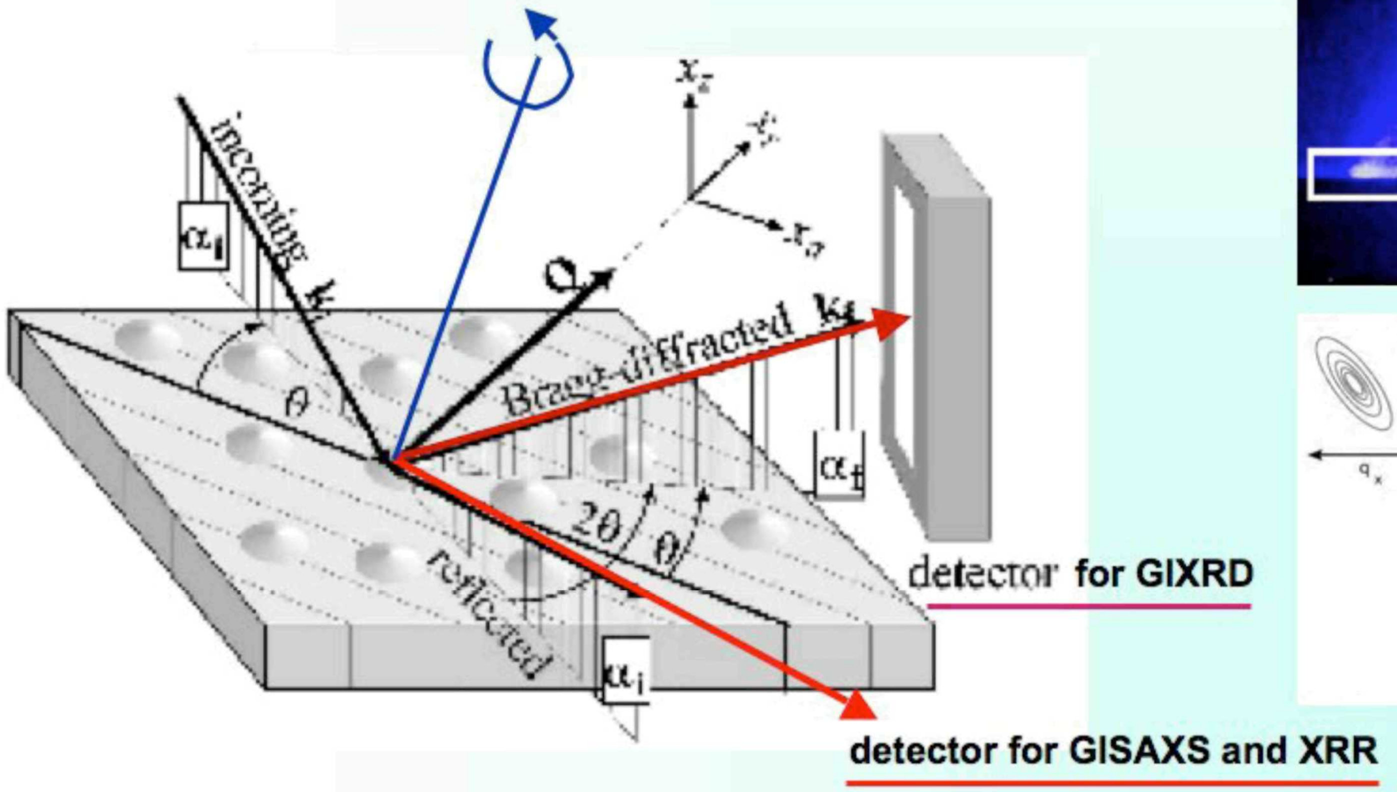


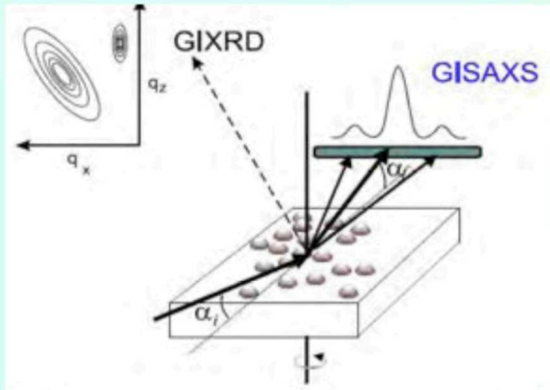

# Grazing Incidence Diffraction (GID)

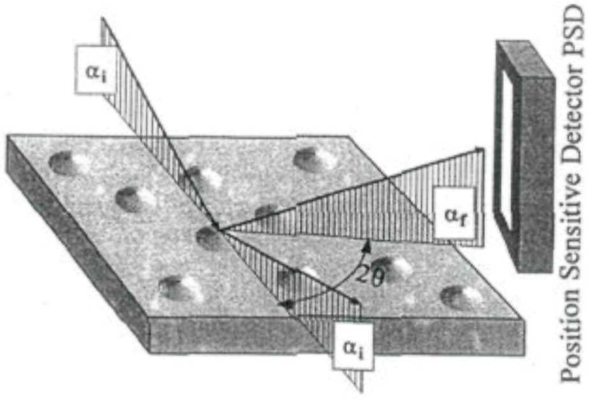


Scattering geometry for grazing incidence diffraction to study the crystalline properties of quantum dots. Three-dimensional reciprocal space maps are recorded in this geometry by collecting the scattered intensity as a function of the exit angle $\alpha_f$, the scattering angle $2\theta$ and the sample angle $\theta$.

**InAs islands grown by molecular beam epitaxy on GaAs(100) at 530°C substrate temperature**

**GID -> crystalline properties of coherent quantum dots**

**Analysis of reciprocal space maps -> interdependence of shape and elastic strain within the quantum dots**

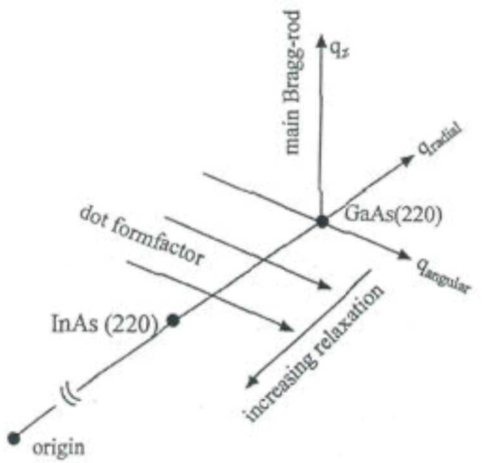


Important directions in reciprocal space close to the (220) surface Bragg reflections of GaAs and InAs. By adjusting $q_r$ the lattice relaxation in the dots is measured, along $q_a$ information on the lateral form factor of the dots is obtained, the $q_z$-dependence determines the maximum depth and reveals the form factor of the dots in the growth direction.

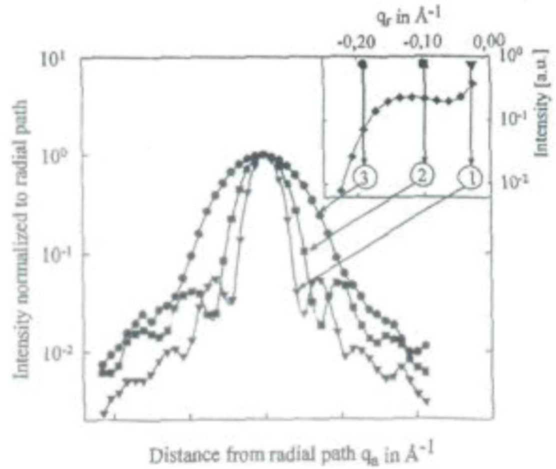


'Isostrain-scattering' between the (220) surface Bragg reflections of GaAs and InAs. The intensity distribution in angular scans is shown for different radial positions ($q_r$) as indicated in the inset. The angular dependence ($q_a$) of the scattering signal is characteristic for the lateral shape of the InAs dots. The central maximum broadens with increasing relaxation $|q_r|$

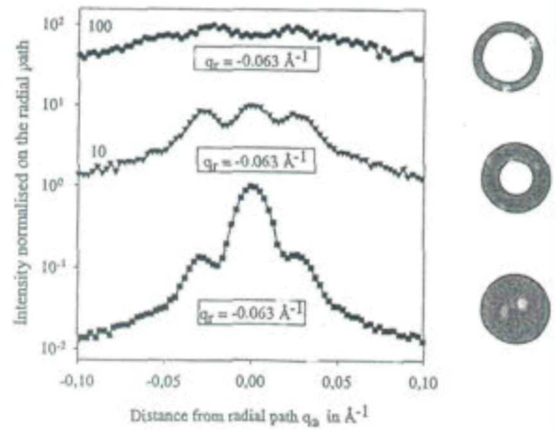


Form factor-induced scattering signal as a function of $q_a$ for ring-shaped InAs islands overgrown by GaAs as a function of the relaxation $q_r$. The corresponding shapes of the islands are indicated schematically on the right-hand side.

**T.H. Metzger et. al., J. Phys. D.: Appl. Phys. 32 (1999) A202-A207**

# X-ray Reflectivity measurements

**Determine**

- **Surface / interface roughness**
- **Layer thickness**

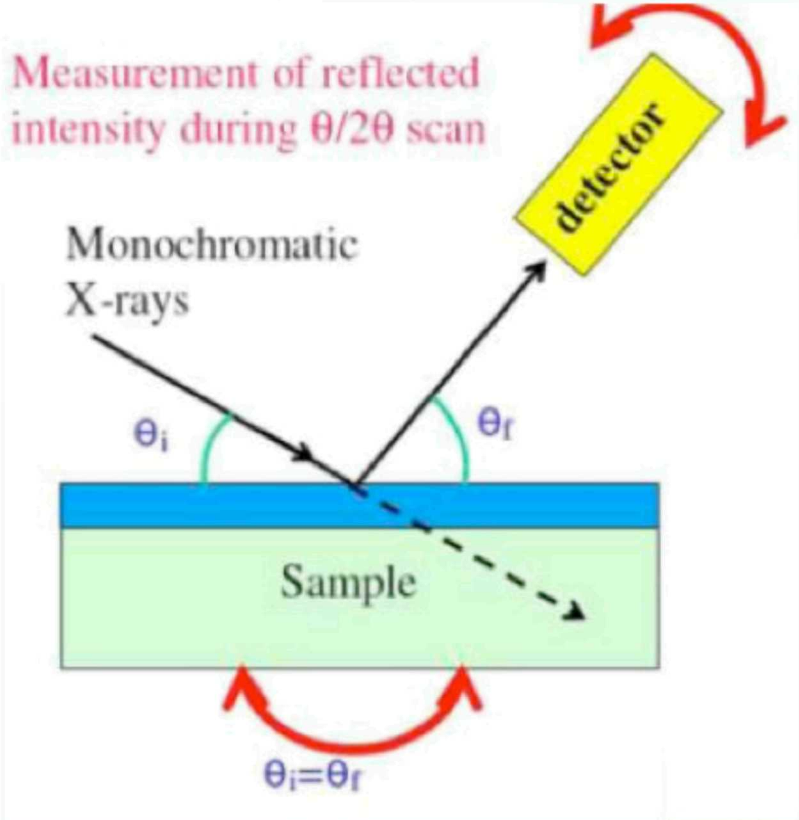


**Why layer thickness ?**

**Because function of devices depends on thickness:**

- **IC (semiconductors)**
- **Solar cells (photovoltaic materials)**
- **Displays (liquid crystals)**
- **Data storage (magnetic multilayer)**
- **Biomaterial (proteins, lipids -> biochip)**
- **LED (electroluminescence)**
- **Coatings and platings (optical materials)**

# X-ray Reflectivity measurements

## Thin films on substrates:

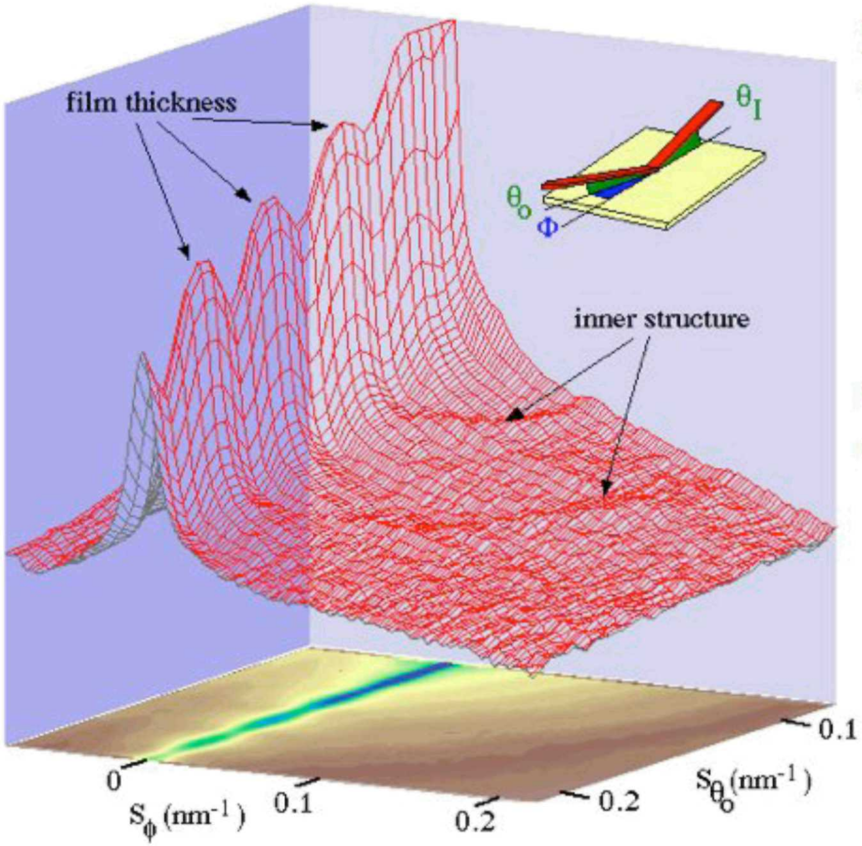


**high correlation between the film and substrate surface**

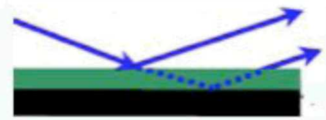

**➔ interference patterns in the specular plane**
**➔ precise film thickness determination**

**concentric rings around the direct beam direction correspond to inner structure of the film**

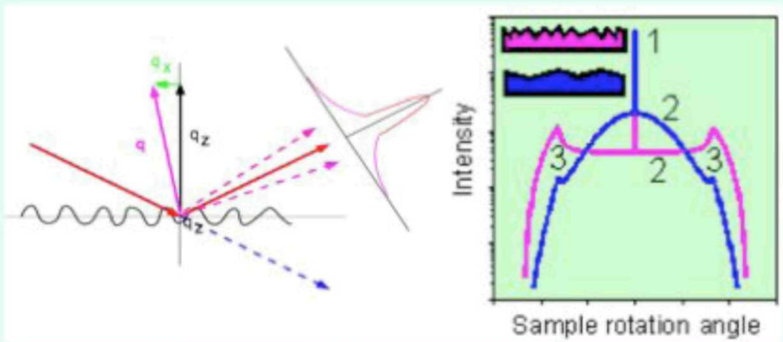


**Rough surfaces -> diffuse scattering**
**-> lateral features of the roughness: height-height correlations**

# Basic experimental considerations

High photon flux is needed for GI-scattering: Nr. of atoms in interfaces / surfaces is << as in bulk ! -> use rotating anodes or synchrotron sources !

Critical angles for e.g. 8 kV photons:

| | |
|---|---|
| organic films | ac = 0.1° <-> 1.7 mrad |
| substrates | ac = 0.2° <-> 3.4 mrad |

--> • very flat substrates needed (e.g. silicon wafers, float glass)

• very flat films (spin coating, dip coating, implanting, ...) needed

Sample size (length L x width W):

accepted beam height H = L x a

L= 20 mm, a = 0.2° -> H = 70 mm

W > beam width of ca. 5 mm

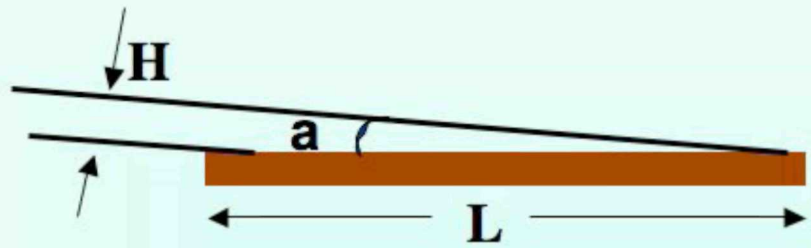


Sample surrounding

avoid photons scattered from air -> work in vacuum, He-atmosphere, or use very short air-paths

avoid photons scattered from slits, windows, ...

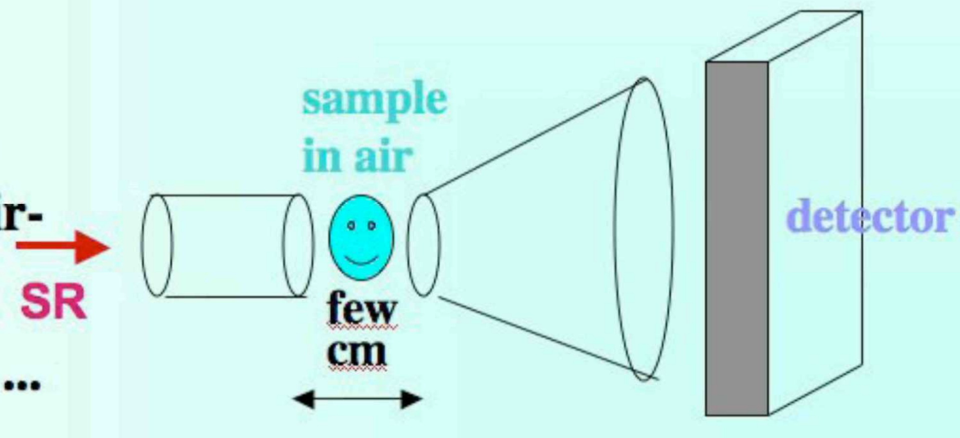

# GISAXS is an ideal tool to study:

- non-destructive
- no special sample preparation / samples as prepared (implanted, spin / dip coating, …)
- in ambient conditions, or under vacuum
- mesoscopic scale: from molecular size to ca 150 nm
- extremely sensitive to lateral and normal structure
- accurate statistical average
- compatible with in-situ experiments (parameters can be temperature, shear, tear, chemical mixing, …)
- Low-contrast systems possible
- very weakly-scattering samples possible (probe shape and 2D organization of interfaces and QD, of biological molecules deposited on surfaces - > bio-chips, function of selected bio-molecules)

**ESSENTIAL**

- source providing high flux / brilliance
- 2D detector with high dynamic range, and very low background / noise

# Thank you for your attention !

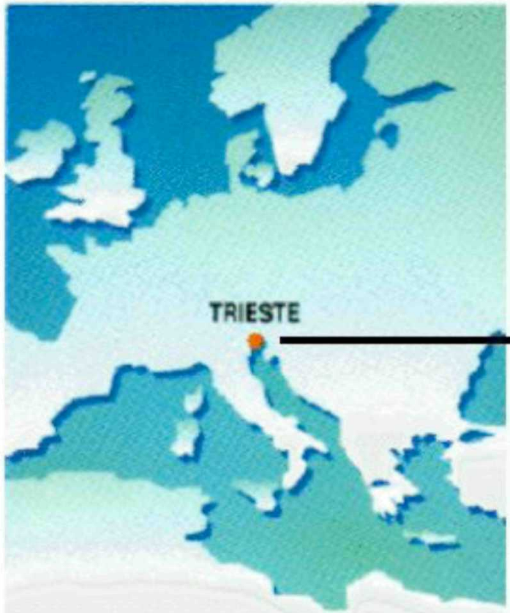


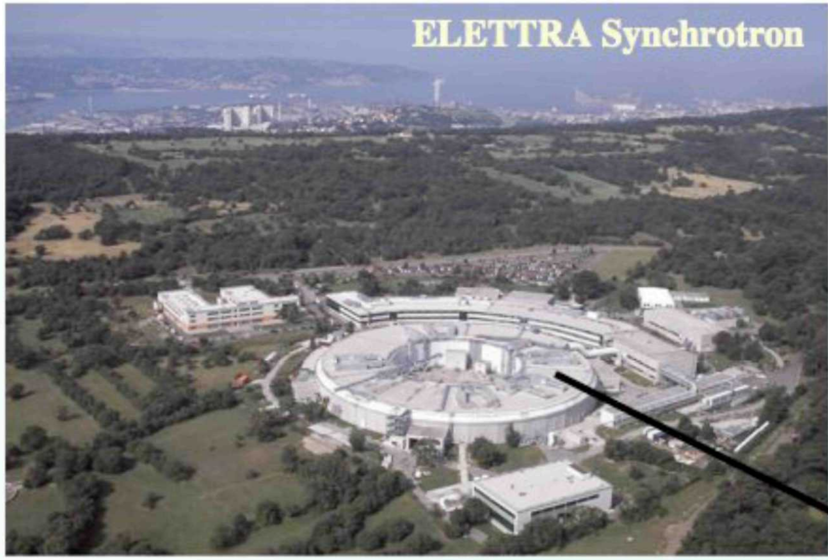


SAXS beamline


If you now want to perform your own SAXS or GISAXS experiment with SR:

Info: www.elettra.trieste.it
www.ibn.oeaw.at/beamline/

you are also welcome to e-mail me at

bernstorff@elettra.trieste.it

# Some useful literature ...

## SAXS:


- A. Guinier and G. Fournet, "Small-Angle Scattering of X-rays", Wiley, New York, 1955
- O. Glatter and O. Kratky, editors of "Small-Angle X-Ray Scattering", Academic Press, New York 1982
- L. Feigin and D. Svegun, "Structure Analysis by Small-Angle X-Ray and Neutron Scattering, Plenum Press, New York, 1987
- O. Kratky and P. Laggner, "X-Ray Small-Angle Scattering", Encyclopedia of Physical Science and Technology, Vol 17, pp. 727-781, Academic Pres, Orlando, 1992
- H. Brumberger, editor of "Modern Aspects of Small-Angle Scattering", NATO Advanced Series, Kluwer, Dordrecht, 1993
- Manfred's homepage http://scattering.tripod.com/


## GISAXS:


- T H Metzger, I Kegel, R Paniago and J Peisl," Grazing incidence x-ray scattering: an ideal tool to study the structure of quantum dots", J. Phys. D: Appl. Phys. 32 (1999) A202-A207
- Till Hartmut Metzger, Tobias Urs Schuelli and Martin Schmidbauer, "X-ray Methods for Strain and Composition Analysis in Self-Organized Semiconductor Nanostructures", lab-neel.grenoble.cnrs.fr/pageperso/fruche/crphys/contrib/metzger.pdf
- Lazzari R., IsGISAXS: a program for grazing-incidence small-angle X-ray scattering analysis of supported islands, J. Appl. Cryst. 35, (2002) 406.
- Salditt T., Metzger T.H. and Peisl J., Kinetic Roughness of Amorphous Multilayers Studied by Diffuse X-Ray Scattering, Phys. Rev. Lett. 73, (1994) 2228.
- Vineyard G. H., Grazing-incidence diffraction and the distorted-wave approximation for the study of surfaces, Phys. Rev. B 26, (1982) 4146.
- M. Rauscher, T. Salditt and H. Spohn, Phys. Rev. B 52, 16855 (1995)
- M. Rauscher et al., J. Appl. Phys. 86 (12), 6763 (1999)


**Infos on Austrian SAXS beamline at ELETTRA: http://www.ibn.oeaw.ac.at/beamline/**